Nuclear Physics B227 (1983) 221-236

ON INVESTIGATING THE STRUCTURE OF HADRONS: LATTICE MONTE CARLO MEASUREMENTS OF COLOUR MAGNETIC AND ELECTRIC FIELDS AND THE TOPOLOGICAL CHARGE DENSITY INSIDE GLUEBALLS

K. ISHIKAWA

City College, CUNY, New York, USA

G. SCHIERHOLZ

II. Institut für Theoretische Physik der Universität Hamburg, W. Germany

H. SCHNEIDER

Deutsches Elektronen-Synchrotron DESY, Hamburg, W. Germany

M. TEPER

LAPP, Annecy

Received 3 January 1983
(Revised 3 June 1983)

We present some techniques for elucidating hadronic structure via lattice Monte Carlo calculations. Applying these techniques, we measure the fluctuations of colour magnetic and electric fields as well as the topological charge density inside and outside the lowest lying 0^+ and 2^+ glueballs in the SU(2) non-abelian lattice gauge theory. This gives us a picture of the glueball structure. We also obtain, as a by-product, an estimate of the gluon condensate $(\alpha_s/\pi)\langle\Omega|F^a_{\mu\nu}F^a_{\mu\nu}|\Omega\rangle$ and an estimate of the 0^- glueball mass which agrees with our previous estimates.

1. Introduction

Recent months have seen considerable progress in calculating the mass spectrum of QCD. Monte Carlo techniques [1] applied to the lattice regulated [2] non-abelian gauge theory have yielded glueball mass estimates for both SU(2) [3-6] and SU(3) [7,8]; and, in the approximation of none or only some quark loops, attempts at calculating the usual meson and baryon masses have also been presented [9-11].

In this paper we wish to go a step further and discuss how to elucidate the internal structure of hadrons in the context of a lattice Monte Carlo approach. As a first example we shall calculate the fluctuations of the colour magnetic and colour electric fields, $\boldsymbol{B}^2$ and $\boldsymbol{E}^2$, as well as the square of the topological charge density, $\sim(\boldsymbol{E}\cdot\boldsymbol{B})^2$, inside the 0^+ and 2^+ glueballs. We work with the pure SU(2) gauge theory on an 8^4 lattice which turns out to be large enough for this purpose. For comparison we shall also calculate the above quantities in the vacuum which, as a by-product, will lead us to an accurate estimate of the gluon condensate $(\alpha_s/\pi)\langle\Omega|F^a_{\mu\nu}F^a_{\mu\nu}|\Omega\rangle$.

Let $|G(x)\rangle$ be the state consisting of the glueball G centred on the space-time point x. Let $\psi(y)$ be an operator with which we wish to probe the structure of G. Then we are interested in measuring

$$\psi_{\mathrm{G}}(x-y)=\frac{\langle G(x)|\psi(y)|G(x)\rangle}{\langle G(x)|G(x)\rangle}\,. \tag{1}$$

Clearly

$$\psi_{\mathrm{G}}(x-y)\underset{|x-y|\to\infty}{\longrightarrow}\langle\Omega|\psi|\Omega\rangle\,, \tag{2}$$

where $|\Omega\rangle$ is the vacuum, and this is also a quantity of interest. Varying y relative to x allows us to probe the glueball at various points in its interior. On a lattice of spacing a any operator will have an extension at least equal to a. So for the glueball to have a structured interior at all, one would want the glueball size, l_{G}, to be at least two lattice spacings across

$$l_{\mathrm{G}}\gtrsim 2a\,. \tag{3}$$

In our previous work [3,4] on glueball masses we obtained a crude estimate of l_{G}. Using that estimate we can restate (3) in terms of the inverse coupling β ($\equiv 4/g^2$) as

$$\beta\gtrsim 2.3\,, \tag{4}$$

(interpreting (3) generously). Since the construction of $|G\rangle$ becomes harder as the lattice spacing decreases, we shall perform our explicit calculations mostly at $\beta=2.3$.

To construct $|G(x)\rangle$ we note that any operator $\phi(x)$ with the same quantum numbers as G will have an expansion of the type

$$\phi(x)|\Omega\rangle=\sqrt{\alpha}\,|G(x)\rangle+\sum_{\nu\neq G}\sqrt{\alpha_\nu}\,|\nu\rangle\,, \tag{5}$$

where in general $\alpha>0$, and if $\langle\Omega|\phi|\Omega\rangle=0$, G will be the lowest energy state in the expansion (we assume that we are interested in the lowest lying glueballs only). We can vary ϕ and search for an operator for which $\alpha=1$ in (5). To do this systematically, one simply searches for the ϕ that will minimise the quantity

$$\frac{\langle\phi(t+a,\boldsymbol{x})\phi(t,\boldsymbol{x})\rangle}{\langle\phi(t,\boldsymbol{x})\phi(t,\boldsymbol{x})\rangle}=\frac{\langle\phi(t,\boldsymbol{x})\mathrm{e}^{-Ha}\phi(t,\boldsymbol{x})\rangle}{\langle\phi(t,\boldsymbol{x})\phi(t,\boldsymbol{x})\rangle}, \tag{6}$$

as in the variational part of the calculations of refs. [3–8]. In practice, however, such an approach only works well at the lowest values of β. At $\beta=2.3$ the simplest implementation of such an approach already breaks down (see for example the results presented in ref. [6]).

An alternative approach is to use some reasonable operator and to project out the required state by introducing a time separation in the glueball states as follows:

$$\frac{\langle\Omega|\phi(t+a,\boldsymbol{x})\psi(t,\boldsymbol{y})\phi(t-a,\boldsymbol{x})|\Omega\rangle}{\langle\Omega|\phi(t+a,\boldsymbol{x})\phi(t-a,\boldsymbol{x})|\Omega\rangle}=\frac{\sum_{n,m}a_n a_m\mathrm{e}^{-E_n a}\mathrm{e}^{-E_m a}\langle n|\Psi|m\rangle}{\sum_n a_n^2\mathrm{e}^{-2E_n a}}$$

$$\approx\frac{\langle G(t,\boldsymbol{x})|\psi(t,\boldsymbol{y})|G(t,\boldsymbol{x})\rangle}{\langle G(t,\boldsymbol{x})|G(t,\boldsymbol{x})\rangle}, \tag{7}$$

where the accuracy of the last equality will depend on the efficiency with which the

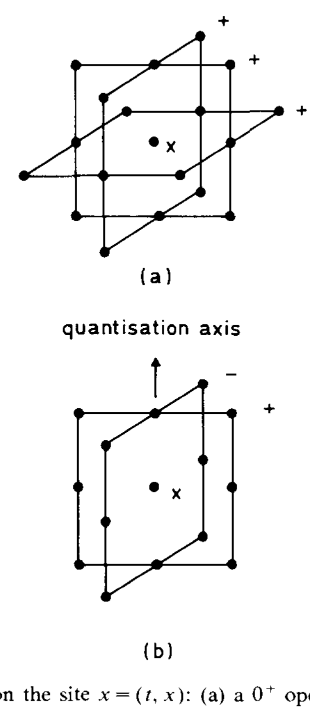

Fig. 1. Glueball operator centred on the site $x=(t,\boldsymbol{x})$: (a) a 0^+ operator that is the sum of the three orthogonal 2×2 plaquettes, (b) a 2^+ operator that is the difference of an orthogonal pair of 2×2 plaquettes.

energy exponentials project out the lowest energy state. Our previous experience [3,4] has been that at $\beta = 2.3$ the projection is indeed efficient. Increasing the time separation makes (7) more accurate. However, the reduced signal can very rapidly disappear into the statistical noise. In order to overcome this, and still making advantage of the more effective projection onto the lowest-lying glueballs by introducing a time separation, we shall later on also use $\Delta t = a$ time separations where the probe sits at the same time as one of the glueballs.

A simple pair of 0^+ and 2^+ operators are shown in fig. 1. They consist of 2×2 plaquettes centred at the site $(t, \boldsymbol{x})$ and in the appropriate linear combination for the desired spin and parity. The corresponding 2^+ has spin projection $J_3 = \pm 2$. From our previous work [4] (fig. 8) we learn that $\alpha \approx 0.5$ (at $\beta = 2.3$ where most of our data comes from). This is to say that the 2×2 plaquette has a $\approx 50\%$ projection onto the lowest-lying glueballs, so that already zero time separation will give us some picture of the glueball ground states.

2. Vacuum fluctuations: a re-evaluation of $(\alpha_s/\pi)\langle\Omega|F^a_{\mu\nu}F^a_{\mu\nu}|\Omega\rangle$

Before we turn to probe the structure of the 0^+ and 2^+ glueballs with colour magnetic and colour electric fields, i.e.

$$\psi(y) = B_i^2(y) \underset{i \neq j \neq k = 1,2,3}{=} F^a_{jk}F^a_{jk}(y) \underset{(a \to 0)}{=} 4a^{-1}\beta\left(1 - \tfrac{1}{2}\mathrm{tr}\, U_{jk}\right), \tag{8}$$

$$\psi(y) = E_i^2(y) = F^a_{4i}F^a_{4i}(y) \underset{(a \to 0)}{=} 4a^{-1}\beta\left(1 - \tfrac{1}{2}\mathrm{tr}\, U_{4i}\right), \tag{9}$$

where

$$U_{\mu\nu}(y_n) = U_\mu(y_n)U_\nu(y_n + \mu)U_\mu^\dagger(y_n + \nu)U_\nu^\dagger(y_n), \tag{10}$$

which on the lattice are formally given by the space- and time-like plaquettes as indicated, we shall have to evaluate the above quantities in the vacuum. There are two reasons for that. First of all, the expectation value of the simple plaquette is, for $\beta \gtrsim 2.3$, overshadowed by its perturbative contribution which must be subtracted out to recover the continuum limit. This requires to measure the average plaquette over a wide range of β values. And secondly, we have a natural interest in the confining vacuum itself in which the hadrons are immersed.

This leads us to study the vacuum expectation value of $1 - \frac{1}{2}\mathrm{tr}\, U_{\mu\nu}$ which can be written

$$\langle\Omega|\left(1 - \tfrac{1}{2}\mathrm{tr}\, U_{\mu\nu}\right)|\Omega\rangle = \sum_{n=1}^{\infty} c_n\beta^{-n} + \tfrac{1}{24}\pi^2 a^4 G,$$

$$G = \frac{\alpha_s}{\pi}\sum_{a,\mu\nu}\langle\Omega|F^a_{\mu\nu}F^a_{\mu\nu}|\Omega\rangle, \tag{11}$$

where G, the so-called gluon condensate, is a renormalization group invariant. The first two coefficients c_1 and c_2 in the series of (11) have been determined analytically [12, 13] and are given by

$$c_1 = 0.75\,, \qquad c_2 = 0.1518 \text{ on } 8^4\,. \tag{12}$$

Preliminary results on (11) obtained on a rather small 4^4 lattice have been reported in the literature [13]. We find it necessary, however, to repeat the analysis on the 8^4 lattice because already at $\beta = 2.5$ the 4^4 lattice corresponds to a temperature well above the deconfining phase transition. As a result we expect G to come out larger on a larger lattice.

We have taken data in the range $2.3 \leqslant \beta \leqslant 8.0$. For $\beta \geqslant 2.9$ the full SU(2) group was used while for $\beta < 2.9$ we also have made use of the 120 element icosahedrical subgroup of SU(2) which was found to give results in very good agreement with the full group. Our combined data is listed in table 1.

In fitting (11) to our data we have allowed for terms up to order β^{-5} in the series. Leaving all coefficients free first we obtain, as a check, for $\beta \geqslant 2.9$

$$c_1 = 0.748\,, \qquad c_2 = 0.195\,, \tag{13}$$

in good agreement with the analytic result (12). In the actual fit then we have fixed c_1 and c_2 at their analytic values and covered the full β range ($2.3 \leqslant \beta \leqslant 8.0$). The

TABLE 1
Our combined data for the vacuum expectation value of the 1×1 plaquette over the range $2.3 \leqslant \beta \leqslant 8$

β	$\langle \Omega \vert \frac{1}{2} \mathrm{tr}\, U_{\mu\nu} \vert \Omega \rangle$
2.3	0.60277 ± 0.00014
2.4	0.63067 ± 0.00016
2.5	0.65245 ± 0.00012
2.6	0.67026 ± 0.00017
2.7	0.68560 ± 0.00018
2.8	0.69952 ± 0.00018
2.9	0.71223 ± 0.00015
3.2	0.74296 ± 0.00017
3.5	0.76780 ± 0.00011
4.0	0.79965 ± 0.00012
5.0	0.84244 ± 0.00009
6.5	0.88040 ± 0.00006
8.0	0.90356 ± 0.00005

Each entry is based on 1000–2000 events for $\beta < 2.9$ and on ≈ 300 events for $\beta \geqslant 2.9$.

outcome is:

$$c_3 = 0.26\,, \qquad (c_4 = -0.84\,, \qquad c_5 = 2.63)\,, \tag{14}$$

$$G = (2.1 \pm 0.1) \cdot 10^7 \Lambda_{\mathrm{L}}^4\,. \tag{15}$$

The brackets around c_4 and c_5 in (14) mean that these coefficients are not very well determined by the fit and are also not very relevant to the determination of G (see below). In fig. 2 we have shown the resulting perturbative contribution subtracted data for

$$\Delta = \langle \Omega | \left(1 - \tfrac{1}{2} \operatorname{tr} U_{\mu\nu}\right) | \Omega \rangle - \sum_{n=1}^{5} c_n \beta^{-n} = \tfrac{1}{24} \pi^2 a^4 G\,, \tag{16}$$

together with the best fit (15), where a is approximated by the two-loop formula

$$a = \Lambda_{\mathrm{L}}^{-1} \mathrm{e}^{-3\pi^2 \beta/11} \left(6\pi^2 \beta/11\right)^{51/121}. \tag{17}$$

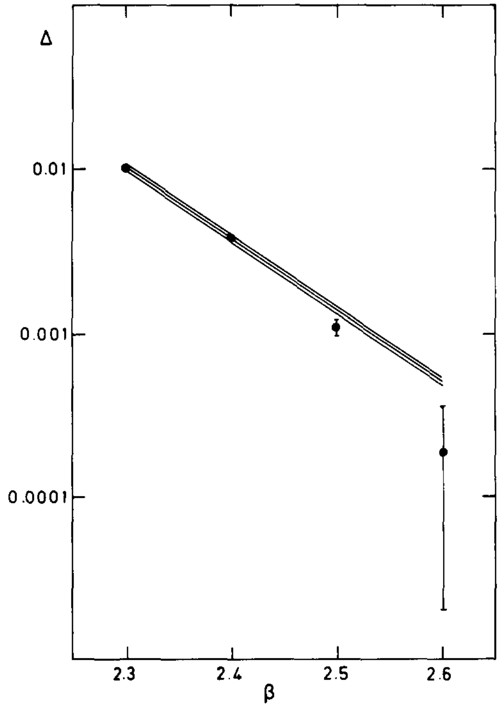

Fig. 2. The gluon condensate (16) for various values of β. The middle line corresponds to our best fit while the lines above and below indicate the error.

The rather large coefficients c_4 and c_5 might lead one to suspect that the fit depends crucially on the order of truncation of the perturbative series. This is not the case. First of all, we like to say that at large β, where the perturbative contribution dominates, the terms of $O(\beta^{-4})$ are small, while at smaller β the *sum* $c_4\beta^{-4} + c_5\beta^{-5}$ contributes at most 2% to the perturbative series. Secondly, we have fitted our data by truncating the perturbative series only after the 6th order. We obtain basically the same result for G. In fact, we have made the variations of G found by our various fits (with comparable χ^2/(degree of freedom)) the basis of our error estimate in (15). Furthermore, the coefficients c_4 and c_5 come out somewhat smaller which indicates that their magnitude is an artifact of the truncation. We have also tried to fit the data setting $G = 0$ and obtain $\chi^2 = 63.7$/(degree of freedom) while our best fit gives $\chi^2 = 1.8$/(degree of freedom).

Our result for the condensate (15) is 50% higher than that on the 4^4 lattice which is quite understandable. It is also not surprising that the condensate falls below the fitted value at higher values of β (fig. 2). Using our measured value of the string tension [3], $\Lambda_L = 0.012 \cdot \sqrt{K}$, and assuming $\sqrt{K} = 400$ MeV (corresponding to unit Regge slope) we obtain in absolute units

$$G = (11.1 \pm 0.6)\ 10^{-3}\ \mathrm{GeV}^4 = (325 \pm 16\ \mathrm{MeV})^4. \tag{18}$$

3. Probing the glueballs with colour magnetic and colour electric fields

Let us first concentrate on probing the interior of the glueballs with the colour magnetic field. To do so, the probe has been placed at various positions relative to the centre of the glueballs as indicated in fig. 3. We have taken data, $\simeq 6000$ events in all, for $\Delta t = 0$, $\Delta t = a$ and $\Delta t = 2a$ time separations in the glueball states (cf. (7)). The $\Delta t = 2a$ data are, however, not very conclusive yet as the errors are still too large. The perturbative contribution to the expectation values of the various plaquettes has been subtracted out in the form of our polynomial fit (14). The square root of the resulting ratios, $[\langle G|\boldsymbol{B}^2|G\rangle / \langle \Omega|\boldsymbol{B}^2|\Omega\rangle]^{1/2}$, is shown in figs. 4–6 as a function of the distance from the centre of the glueballs. We have associated $\boldsymbol{B}^2$ with the centre of the plaquettes and allowed for a displacement of $\frac{1}{4}a$ in both directions which is indicated by the horizontal error bars. To convert the distance into fm we have used (17) and our measured Λ_L. It is to be noted that figs. 4–6 contain data at both $\beta = 2.3$ and $\beta = 2.5$ which, at least for $\Delta t = 0$, will have a different admixture of excited states. This one should bear in mind in comparing the two sets of data.

From fig. 4 we infer that the 0^+ glueball is densely packed with colour magnetic fields, and that the diameter of the 0^+ glueball is about 0.5 fm. Roughly the same picture arises for the 2^+ glueball. It has, however, a richer structure as can be inferred from the two cross sections perpendicular and parallel to the quantisation axis shown in figs. 5 and 6, respectively. To make the structure of the 2^+ glueball more apparent, we have rotated the colour magnetic fields located at the centre of

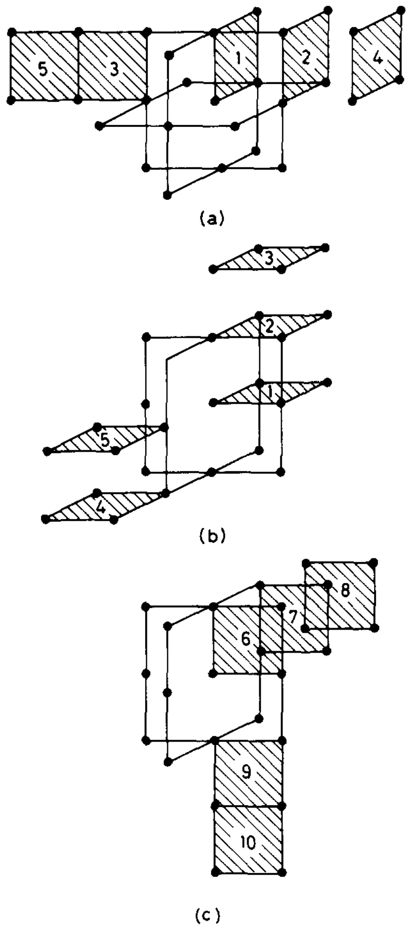

Fig. 3. Placement of space-like plaquettes relative to the glueball centre: (a) 0^+, (b) and (c) 2^+.

the plaquettes in figs. 3a, b around the quantisation axis into one plane, making use of the rotational invariance of the glueball state, and obtain the equi-potential contour plot shown (for our $\Delta t = 0$ data) in fig. 7. This resembles two constituent vector gluons sitting in the two centres with their spins aligned and spin projection $J_3 = \pm 2$. In order that this can be realized quantum-mechanically, the constituent gluons have to be in a relative $L = 2$, $L_3 = 0$ wave. The distance between the two constituent gluons is roughly 0.15 fm. This will be of particular interest for the glueball phenomenology.

Let us now turn to probing the glueballs with the colour electric field. We have placed the probe, a time-like plaquette in this case, as indicated in fig. 8 and taken data for $\Delta t = 0$, $\Delta t = a$ and $\Delta t = 2a$ time separations. Due to large errors the $\Delta t = 2a$

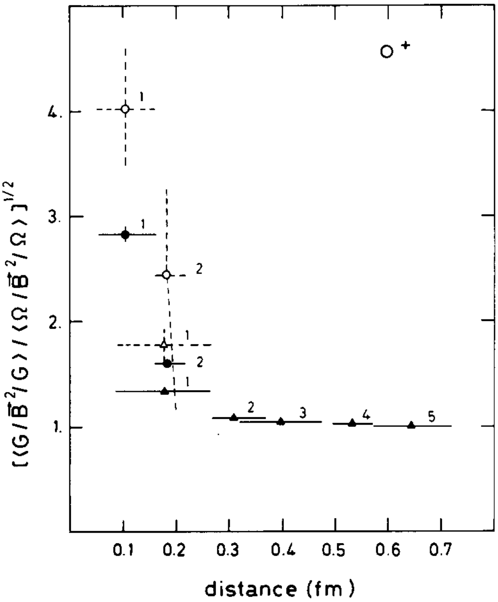

Fig. 4. Cross section of the 0^+ glueball. The closed (open) triangles correspond to $\beta = 2.3$, $\Delta t = 0$ ($\beta = 2.3$, $\Delta t = a$) and the closed (open) circles correspond to $\beta = 2.5$, $\Delta t = 0$ ($\beta = 2.5$, $\Delta t = a$). The location of the corresponding plaquettes within the glueball is indicated by the numbers; see fig. 3.

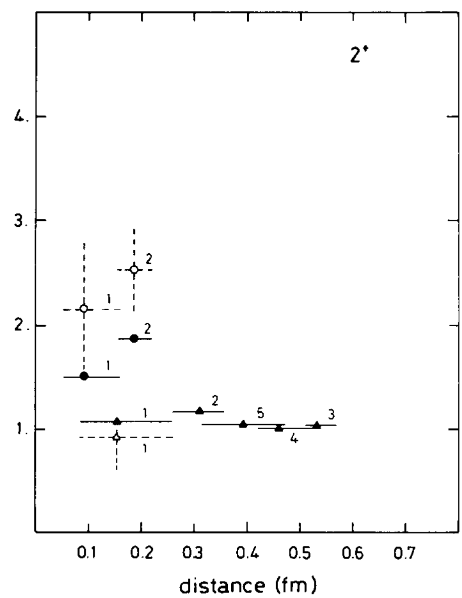

Fig. 5. Cross section of the 2^+ glueball parallel to the quantisation axis. Notation as in fig. 4.

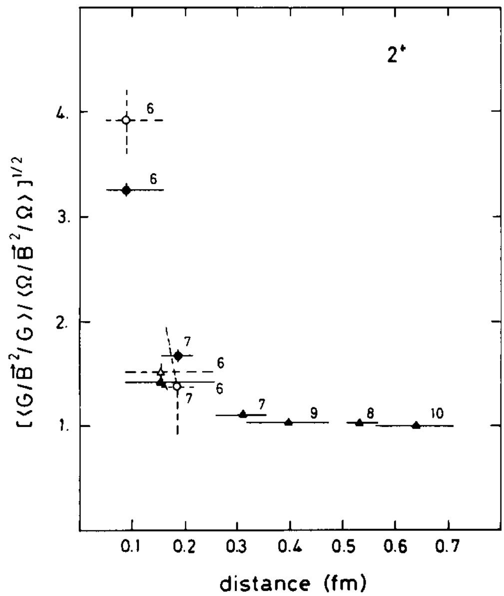

Fig. 6. Cross section of the 2^+ glueball perpendicular to the quantisation axis. Notation as in fig. 4.

data are not very conclusive here as well and will be left out of the discussion. We have subtracted out the perturbative contribution as before and obtain at $\beta = 2.3$, based on a total of 650 events,

$\left[\frac{\langle G\|E^2\|G\rangle}{\langle\Omega\|E^2\|\Omega\rangle}\right]^{1/2}$	$\Delta t = 0$	$\Delta t = a$
0^+	1.09 ± 0.01	1.38 ± 0.06
2^+	1.07 ± 0.01	1.16 ± 0.20

(19)

This gives the same picture as the colour magnetic probe, that is to say the glueballs are strongly excited objects rather than being largely empty.

Altogether we are led to conclude that the condensate G is a factor $\gtrsim 2$ larger inside the glueballs than in the vacuum (which follows from taking the square of the quantities shown in figs. 4–6 and (19)), and that it varies considerably from the 0^+ to the 2^+ glueball. This has some interesting consequences for our understanding of the hadrons and the vacuum. Furthermore, it contradicts the assumption of factorisation which goes into the derivation of the ITEP sum rules [14].

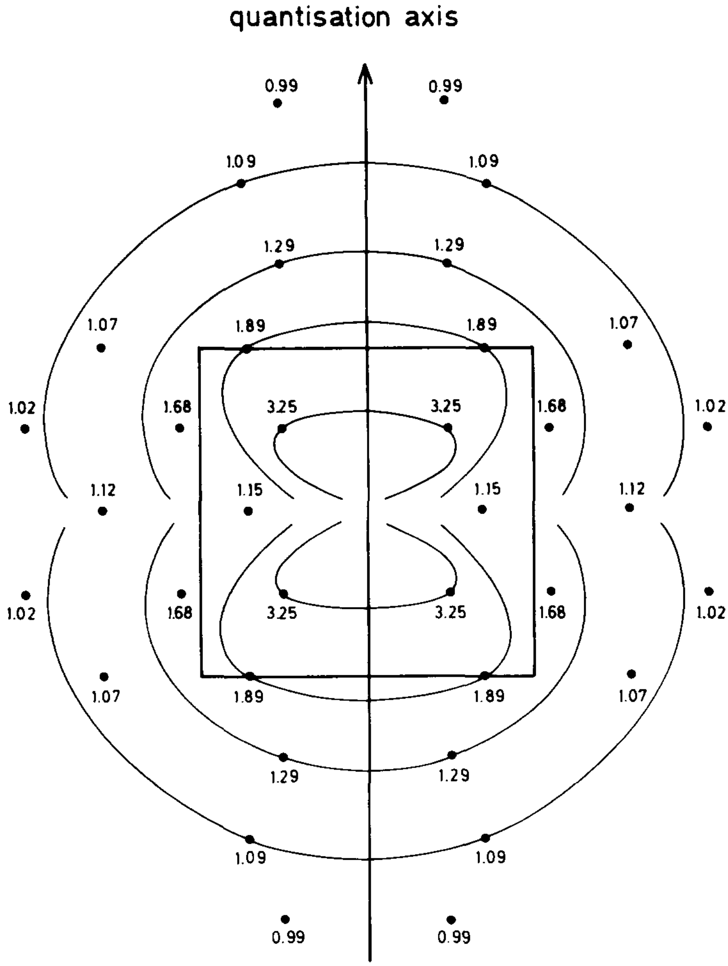

Fig. 7. Equi-potential contour plot of the colour magnetic field inside the 2^+ glueball. The dots correspond to the location of the various plaquettes (figs. 3b and c), rotated into one plane. The numbers give the ratios $[\langle 2^+ | \boldsymbol{B}^2 | 2^+ \rangle / \langle \Omega | \boldsymbol{B}^2 | \Omega \rangle]^{1/2}$ for $\beta = 2.5$ and $\Delta t = 0$. Also drawn is the 2×2 plaquette which sets the scale: $2a \approx 0.3$ fm.

4. Probing the glueballs with the topological charge density

We shall now probe the structure of the 0^+ and 2^+ glueballs with

$$\psi(y) = Q^2(y) = \left(\frac{1}{16\pi^2 \beta} \varepsilon_{\mu\nu\rho\sigma} F^a_{\mu\nu} F^a_{\rho\sigma}(y) \right)^2 , \tag{20}$$

where $Q(y)$ is the so-called topological charge density.

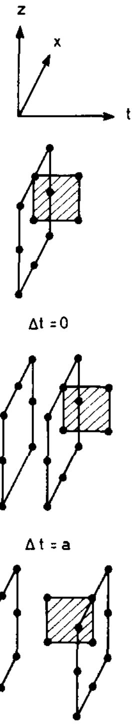

Fig. 8. Placement of the time-like plaquette relative to the glueballs.

The lattice version of $Q(y)$ we begin with is [15]

$$a^4 Q(y) = -\frac{\varepsilon_{\mu\nu\rho\sigma}}{32\pi^2}\operatorname{tr}(U_{\mu\nu}U_{\rho\sigma}), \tag{21}$$

where $U_{\mu\nu}$ is the plaquette (see (10)) obtained by first going in the positive μ direction and then in the positive ν direction, and where y is the point at which the plaquettes $U_{\mu\nu}$ and $U_{\rho\sigma}$ connect. See fig. 9 for a typical contribution. We now extend the sum in (21) to include contributions where we go initially in the negative μ direction etc., so that our operator may have negative parity. To ensure that it possesses appropriate positivity properties [16] we perform this symmetrisation for both time-like and space-like directions. Our final operator thus coincides with one of those defined in ref. [17]:

$$a^4 Q(y) = \sum_{\mu\nu\rho\sigma=\pm 1}^{\pm 4} \frac{\tilde{\varepsilon}_{\mu\nu\rho\sigma}}{2^4 \cdot 32\pi^2}\operatorname{tr}(U_{\mu\nu}U_{\rho\sigma}), \tag{22}$$

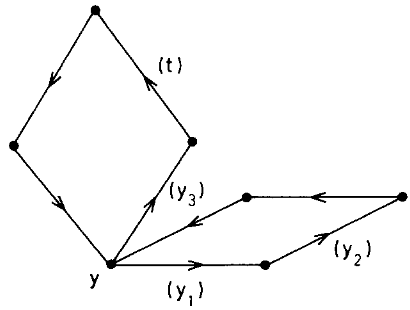

Fig. 9. An eight-link loop that contributes to $Q(y)$. The links are labelled by the directions in which they point.

with $\tilde{\varepsilon}_{1234} = -\tilde{\varepsilon}_{2134} = -\tilde{\varepsilon}_{-1234}$ etc. For SU(2) this may be simplified in practical calculations using the decomposition

$$\begin{aligned}\tfrac{1}{4}\varepsilon_{\mu\nu\rho\sigma}\mathrm{tr}(U_{\mu\nu}U_{\rho\sigma}) = &\{2\,\mathrm{tr}(U_{12}U_{34}) - \mathrm{tr}\,U_{12}\mathrm{tr}\,U_{34}\}\\ &-\{2\,\mathrm{tr}(U_{13}U_{24}) - \mathrm{tr}\,U_{13}\mathrm{tr}\,U_{24}\}\\ &+\{2\,\mathrm{tr}(U_{23}U_{14}) - \mathrm{tr}\,U_{23}\mathrm{tr}\,U_{14}\}\,. \qquad (23)\end{aligned}$$

In our measurements of (22) inside the glueballs we shall place y at the glueball centre, i.e. $y = x$ as indicated in fig. 1.

As in the case of the simple plaquette, the expectation value of (22) is non-zero in perturbation theory. The attitude that we shall also take here is to subtract out the perturbative contribution,

$$\langle\Omega|(a^4Q(z))^2|\Omega\rangle = d_2\beta^{-2} + \mathrm{O}(\beta^{-3})\,, \qquad (24)$$

to estimate the continuum limit.

We have calculated the first coefficient d_2 and obtain

$$d_2 = \frac{9}{512\pi^4}\,. \qquad (25)$$

Going beyond that proves to be a tedious, if not impossible task. One could, alternatively, determine the higher coefficient by measuring the vacuum expectation value (24) over a wide range of β values and fit to it a polynomial plus renormalization group invariant as we did in the case of the plaquette. But this is very time consuming for the operator (22) and the 8^4 lattice we are using. We shall therefore approximate the perturbative contribution by the dominant term in the weak-coupling expansion, $d_2\beta^{-2}$. It also turns out that we need not know the perturbative contribution more precisely for the conclusions we like to draw. This was quite different in the case of the simple plaquette.

We have measured $(a^4Q)^2$ inside the 0^+ and 2^+ glueballs and in the vacuum. Based on 1400 events we obtain, after having subtracted out the perturbative contribution, at $\beta = 2.3$

$\left[\dfrac{\langle G\|Q^2\|G\rangle}{\langle\Omega\|Q^2\|\Omega\rangle}\right]^{1/2}$	$t=0$	$t=a$	$t=2a$
0^+	1.29 ± 0.01	1.61 ± 0.07	1.32 ± 0.30
2^+	1.23 ± 0.01	1.07 ± 0.04	-0.93 ± 0.73

(26)

and $\langle\Omega|(a^4Q)^2|\Omega\rangle = (6.03 \pm 0.01)10^{-6}$. The ratios of the true non-perturbative values could be much higher. However, already on the basis of (26) we can say that the topological charge density is substantially larger inside the glueballs than in the vacuum.

Naively, this suggests that at least the 0^+ contains a bigger portion of some dilute instanton gas than the vacuum. If instantons are around we would, however, expect to find integral ($\neq 0$) topological charges. We have investigated this [18] but so far have found no indication of instantons in the *vacuum* and at $\beta = 2.3$. This does not contradict the above interpretation. It can well be that scaling sets in somewhat later for instanton related quantities, or that there are no dilute instantons in the physical vacuum. A more detailed investigation is in progress, and we hope to report our findings in the near future.

Before summarising our results we will make a brief digression on the mass of the lowest lying 0^- glueball. The operator Q has 0^- quantum numbers and hence when applied to the vacuum it will generate the lowest mass 0^- glueball state as in (5). We measure (using Q as in (22))

$$\frac{\Gamma_{2a}}{\Gamma_0} \equiv \frac{\langle\Omega|Q(t+a,x)Q(t-a,x)|\Omega\rangle}{\langle\Omega|Q(t,x)Q(t,x)|\Omega\rangle}$$

$$\simeq \alpha \mathrm{e}^{-2aE(0^-)}, \tag{27}$$

where

$$\alpha = \frac{|\langle\Omega|Q|0^-\rangle|^2}{\sum_n |\langle\Omega|Q|n\rangle|^2}, \tag{28}$$

and where we expect [3,4] (27) to be a very good approximation. We parametrize

$$E^2 = m^2 + \delta^2/a^2, \tag{29}$$

where δ^2 is the momentum smearing, and (29) should be good for $\delta^2 \ll (ma)^2$ which will be the case here. We also calculate the same quantity using our 2^+ operator. Using the mass estimate [4]

$$m(2^+) \approx 2.46/a, \tag{30}$$

and the wave-function estimate $\alpha \approx \frac{1}{2}$ [4] we obtain

$$\delta^2 \approx 1.5. \tag{31}$$

We do not know α for the 0^- glueball, but most of the variation in (27) is provided by the exponential, so our calculation is insensitive to moderate variations in α. Using $\alpha = \frac{1}{2}$ and (31) then gives us

$$m(0^-) \approx 2.8/a. \tag{32}$$

We can also repeat the calculation using for our wave function in (27) not just Q at one site but summing over neighbouring sites, so that the momentum smearing, δ^2, is reduced. We obtain

$$m(0^-) \approx (2.3 \pm 0.4)/a, \tag{33}$$

where the error corresponds to ranging α between 0.25 and 1. Our conclusion that

$$m(0^-) \approx m(2^+), \tag{34}$$

confirms our previous results [3] performed with different operators on smaller lattices.

5. Summary

We have probed the structure of the 0^+ and 2^+ glueballs with colour magnetic and colour electric fields as well as the topological charge density. The difference found between placing the probe inside and outside the glueballs demonstrates that even with such a course discretisation of space-time as employed here, the glueballs retain enough structure to make their detailed investigation feasible.

The physical picture which emerges is that the 0^+ and 2^+ glueballs are visibly extended objects with a diameter of ≈ 0.5 fm. The 0^+ appears to be a ball with increasing field strength towards the origin, while the 2^+ indicates two constituent gluons. By comparing our $\Delta t = 0$ and $\Delta t = a$ data we also begin to see the structure of the radially excited glueball states which seem to be largely empty near the origin. As far as probing the dynamical properties of hadrons, like the effect of instantons, which are eventually responsible for confinement, is concerned, a lot remains to be done. But we are confident that the lattice will help to settle these questions.

As a by-product we have obtained a reliable estimate of the gluon condensate, a fundamental parameter of the QCD vacuum.

The computer calculations were performed at the DESY computer centre. One of us (M.T.) thanks T. Walsh for the frequent hospitality and financial support of the DESY theory group and the Institute of Theoretical Science at the University of Oregon for its hospitality during part of this work; this work was supported in part by the US Department of Energy under contract number DE-AT06-76ER70004.

References

[1] M. Creutz, Phys. Rev. Lett. 43 (1979) 553;
K.G. Wilson, Proc. of the 1979 Cargèse Summer Institute
[2] K.G. Wilson, Phys. Rev. D19 (1974) 2445
[3] K. Ishikawa, G. Schierholz and M. Teper, Phys. Lett. 110B (1982) 399; DESY preprint 83-004 (1983), Z. Phys. C, to be published
[4] K. Ishikawa, G. Schierholz and M. Teper, Z. Phys. C16 (1982) 69
[5] M. Falcioni, E. Marinari, M.L. Paciello, G. Parisi, F. Rapuano, B. Taglienti and Zhang Yi-cheng, Phys. Lett. 110B (1982) 295
[6] B. Berg, A. Billoire and C. Rebbi, Ann. of Phys. 142 (1982) 185
[7] K. Ishikawa, G. Schierholz and M. Teper, Phys. Lett. 116B (1982) 429; 120B (1983) 387
[8] B. Berg and A. Billoire, CERN preprints TH.3230 and TH.3267 (1982)
[9] D. Weingarten, Phys. Lett. 109B (1982) 57
[10] H. Hamber and G. Parisi, Phys. Rev. Lett. 47 (1981) 1792;
E. Marinari, G. Parisi and C. Rebbi, Phys. Rev. Lett. 47 (1981) 1795;
F. Fucito, G. Martinelli, C. Omero, G. Parisi, R. Petronzio and F. Rapuano, Nucl. Phys. B210[FS6] (1982) 487
[11] A. Hasenfratz, Z. Kunszt, P. Hasenfratz and C.B. Lang, CERN preprint TH.3220 (1982)
[12] A. DiGiacomo and G.C. Rossi, Phys. Lett. 100B (1981) 481
[13] A. DiGiacomo and G. Paffuti, Phys. Lett. 108B (1982) 327
[14] M. Shifman, A. Vainshtein and V. Zakharov, Nucl. Phys. B147 (1979) 385
[15] M. Peskin, Cornell University preprint CLNS 395 (1978)
[16] M. Lüscher, Comm. Math. Phys. 54 (1977) 283;
K. Osterwalder and E. Seiler, Ann. of Phys. 110 (1978) 440
[17] P. DiVecchia, K. Fabricius, G.C. Rossi and G. Veneziano, Nucl. Phys. B192 (1981) 392; CERN preprint TH.3180 (1981)
[18] K. Ishikawa, G. Schierholz, H. Schneider and M. Teper, to be published